Neurobiology of Aging 81 (2019) 166–176

Contents lists available at ScienceDirect

Neurobiology of Aging

journal homepage: www.elsevier.com/locate/neuaging

Temporal progression of Alzheimer's disease in brains and intestines of transgenic mice

Gunjan D. Manocha [a], Angela M. Floden [a], Nicole M. Miller [a], Abbie J. Smith [a], Kumi Nagamoto-Combs [b], Takashi Saito [c], Takaomi C. Saido [c], Colin K. Combs [a,*]

[a] Department of Biomedical Sciences, University of North Dakota School of Medicine and Health Sciences, Grand Forks, ND, USA
[b] Department of Pathology, University of North Dakota School of Medicine and Health Sciences, Grand Forks, ND, USA
[c] Laboratory for Proteolytic Neuroscience, RIKEN Center for Brain Science, Wako-shi, Saitama, Japan

ARTICLE INFO

Article history:
Received 2 February 2019
Received in revised form 21 May 2019
Accepted 30 May 2019
Available online 13 June 2019

Keywords:
Alzheimer's disease
Transgenic mice
Intestines
APP/PS1
App^{NL-G-F}

ABSTRACT

The amyloid beta (Aβ) peptide is associated with the neurodegenerative and inflammatory changes in brains affected by Alzheimer's disease (AD). We hypothesized that the enteric nervous system also produces Aβ in an intestinal component of disease. To test this idea, we compared C57BL/6 wild-type (WT) male and female mice to two models of Alzheimer's disease, amyloid precursor protein (APP)/presenilin 1 (PS1) mice and amyloid precursor protein NL-G-F (App^{NL-G-F}) mice, at 3, 6, and 12 months of age. Brain Aβ plaque deposition in App^{NL-G-F} mice preceded that in the APP/PS1 mice, observable by 3 months. Three-month-old female App^{NL-G-F} mice had decreased intestinal motility compared with WT and APP/PS1 mice. However, 3-month-old female APP/PS1 mice demonstrated increased intestinal permeability compared with WT and App^{NL-G-F} mice. Both sexes of APP/PS1 and App^{NL-G-F} mice demonstrated increased colon lipocalin 2 mRNA and insoluble Aβ 1–42 levels at 3 months. These data demonstrate an unrecognized enteric aspect of disease in 2 different mouse models correlating with the earliest brain changes.

1. Introduction

Brains affected by Alzheimer's disease (AD) are characterized by robust accumulation of fibrillar amyloid-β (Aβ) peptide containing plaques (Akiyama et al., 1999; Kang et al., 1987). Aβ is proteolytically derived from the amyloid precursor protein (APP). In addition, the fibrillar plaque deposition of Aβ peptide is associated with microglial and astroglial activation (Akiyama and McGeer, 1990; Styren et al., 1990; Wegiel et al., 2001). Therefore, a common disease mechanism suggests a primary neuronal dysfunction with secondary proinflammatory changes (Combs et al., 1999; Perlmutter et al., 1990; Wisniewski et al., 1992). Ideally, earlier diagnosis of disease can allow for timely intervention. However, accurate, early indices of disease rely on brain imaging (Trojanowski et al., 2010; Weiner et al., 2010). An accurate source of peripheral biomarkers, such as from the digestive tract, may provide an inexpensive, additional means of monitoring disease progression.

Although AD produces clear degeneration in the brain, the central nervous system is only one of the intricate nervous systems in the body. Elderly often experience gastrointestinal dysfunction (Camilleri et al., 2008; Everhart and Ruhl, 2009a,b; Johanson et al., 1992; Roach and Christie, 2008; Sonnenberg et al., 1994) and the homology between the enteric and central nervous systems is well known (Goyal and Hirano, 1996; von Boyen et al., 2002). In addition, our prior work as well as that of others has demonstrated expression of APP and its metabolite, Aβ, in enteric neurons and enterocytes (Arai et al., 1991; Galloway et al., 2007; Semar et al., 2013; Shankle et al., 1993; Van Ginneken et al., 2011). In some instances, Aβ-plaque–like deposits have also been shown in mouse and human intestines (Arai et al., 1991; Joachim et al., 1989; Puig et al., 2015a,b). These findings suggest a role for APP expression and metabolism during progression of AD outside the central nervous system.

To better understand whether a gut-brain connection of disease exists, we examined the distal colon as representative of large intestines compared with brains using 2 mouse models of AD, APP/presenilin 1 (PS1) and amyloid precursor protein NL-G-F (App^{NL-G-F}) mice. The APP/PS1 mice express the Swedish mutation in the APP gene and the deltaE9 mutation in the PS1 gene, relying on an ectopic promoter thus leading to supraphysiologic levels of APP. Although these mice demonstrate deposition of plaques and cognitive deficits, they are also known to demonstrate artifacts that are a direct result of APP overexpression (Fukui et al., 2007; Jankowsky et al., 2001, 2004; Nilsson et al., 2014; Reiserer et al., 2007; Saito et al., 2014,

* Corresponding author at: Department of Biomedical Sciences, University of North Dakota School of Medicine and Health Sciences, Grand Forks, ND 58202-9037, USA. Tel.: +7017774025; fax: +7017772382.
E-mail address: colin.combs@und.edu (C.K. Combs).

0197-4580/$ – see front matter © 2019 Elsevier Inc. All rights reserved.
https://doi.org/10.1016/j.neurobiolaging.2019.05.025

2016; Sood et al., 2007). The insertion of transgenes may also disrupt endogenous gene loci in transgenic mice such as APP/PS1, thus presenting a variable phenotype (Saito et al., 2016). As a solution, we elected to use *App*$^{NL-G-F}$ mice that were designed such that mouse APP remains under control of its endogenous promoter, eliminating overexpression of APP (Saito et al., 2014). The APP construct, which contains a humanized Aβ region, includes the Swedish "NL" mutations that promote Aβ production, the Iberian "F" mutation that causes an increase in the Aβ42/Aβ40 ratio, and the Arctic "G" mutation that promotes Aβ aggregation.

Although we and others have examined intestinal pathology in APP/PS1 mice, it has not been explored in the arguably more physiologically relevant *App*$^{NL-G-F}$ mice (Saito et al., 2014). This study was designed to define the nature of any temporal disease presentation in the gastrointestinal system in contrast to the brain to identify whether an enteric aspect of AD exists.

2. Materials and methods

2.1. Animals

App^{NL-G-F} mice (KI:RBRC06344) were obtained from Dr Takashi Saito and Dr Takaomi C. Saido, RIKEN BioResource Center, Japan. These mice have been generated to demonstrate elevated Aβ levels without overexpressing APP. Specifically, the APP construct, which contains a humanized Aβ region, includes the Swedish "NL" mutations that promote Aβ production, the Iberian "F" mutation that cause an increase in the Aβ42/Aβ40 ratio, and the Arctic "G" mutation that essentially promotes Aβ aggregation through facilitating oligomerization and reducing proteolytic degradation. The APP/PS1 transgenic mice [strain 005864 B6.Cg-Tg (APPswe, PSEN1dE9) 85Dbo/Mmjax] and wild-type (WT) mice (C57BL/6) were obtained from the Jackson Laboratory. APP/PS1 expresses the Swedish mutation in APP and dE9 mutation in the PS1 gene, resulting in expression of human APP and secretion of human Aβ. Males and females (n = 10–12) from all 3 strains of mice (C57BL/6 [WT], APP/PS1, and *App*$^{NL-G-F}$) were randomly assigned and then tested for behavior via the cross maze and intestinal activity assays at 3, 6, and 12 months of age before tissue being collected for histochemical, biochemical, and mRNA analyses.

2.2. Animal use

All animal use was approved by the University of North Dakota Institutional Animal Care and Use Committee Protocol 1407-2. Mice were provided food and water *ad libitum* and housed in a 12-hour light/dark cycle. The investigation conforms to the National Research Council of the National Academies Guide for the Care and Use of Laboratory Animals (eighth edition).

2.3. Antibodies and reagents

Primers for real-time PCR were obtained from Invitrogen (ThermoFisher Scientific, Carlsbad, CA). The anti-Aβ (clone D54D2) antibody was obtained from Cell Signaling Technology (Danvers, MA), whereas anti-Aβ antibody (Clone 6E10) was obtained from BioLegend (San Diego, CA). Anti-APP (Y188) antibody was purchased from Abcam (Cambridge, MA). The Aβ 1–40 and Aβ 1–42 enzyme-linked immunosorbent assay (ELISA) kits were obtained from EMD Millipore (Burlington, MA). QIAzol and RNeasy mini kit for RNA isolation were purchased from Qiagen (Germantown, MA) and iTaq Universal SYBR Green One-Step kit was from Bio-Rad (Hercules, CA). FITC-dextran was purchased from Sigma Aldrich (St. Louis, MO). Anti-oligomer (A11) and anti-fibril (OC) antibodies were a kind gift from Prof. Rakez Kayed, University of Texas Medical Branch, Galveston, TX.

2.4. Cross maze

A cross maze apparatus was used to compare working memory between all groups of mice. This protocol allowed mice to explore a cross-shaped maze at their own discretion without any added stress such as lights, sound, food deprivation, and so forth. Male and female C57BL/6 (WT), APP/PS1, and *App*$^{NL-G-F}$ mice at 3, 6, and 12 months of age were placed in the same identical arm of the maze and allowed exploring and choosing additional arms. Timer was set for 10 minutes, and the movement of mice recorded using a camera set atop the maze. Once all 4 feet were within an arm, this was considered a choice. Arm entries were recorded by personnel blinded to the study paradigm. The number of alternations, defined as 4 consecutive entries into 4 different arms, was counted by a separate person, again, blinded to the study parameters, and % alternation for each mouse was calculated as follows: # alternations/(total entries: 3). After 10 minutes of presence in the maze, the mouse was placed back into the cage for 3 days before performing intestinal activity assays.

2.5. Gastric emptying and intestinal transit assay

Motility was assessed as described (Aube et al., 2006). Mice were fasted for 5 hour, orally gavaged with 100 μL of 83 mg/mL 70 kDa FITC-dextran (nonabsorbable) and sacrificed after 30 minutes. The small intestine was divided into 8 segments of equal length. The stomach was taken as segment number 1, and the 8 intestinal segments numbered 2 to 9. Each segment was then flushed with 500 μL phosphate-buffered saline to quantify luminal FITC via a fluorescent plate reader. Gastric emptying was determined by subtracting the dextran remaining in the stomach from the total dextran (in the stomach and small intestine) and dividing this value by total dextran. Intestinal motility/transit was analyzed using the intestinal geometric center (IGC) of the distribution of dextran throughout the intestine and will be calculated following the equation IGC = $\sum$ [(fraction of amount of FITC in each segment) × (segment number)].

2.6. Intestinal permeability

Gut leakiness was quantified by measuring blood levels of a 4 kDa FITC-dextran administered by gavage as described (Aube et al., 2006). Mice were fasted for 2 hours then gavaged with 22 mg/mL FITC-dextran, and blood was collected via cardiac puncture 5 hours later. Dextran levels in the serum were quantified by reading the fluorescence (excitation 480 nm, emission 520 nm) via a fluorescent plate reader (BioTek).

2.7. Immunostaining mouse brains

The paraformaldehyde-fixed right brain hemispheres from 3-, 6-, and 12-month-old male and female C57BL/6 (WT), APP/PS1, and *App*$^{NL-G-F}$ mice were cut using a freezing microtome. Briefly, paraformaldehyde-fixed tissue was embedded in a 15% gelatin (in phosphate-buffered saline) matrix and immersed in a 4% paraformaldehyde solution for 2 days to harden the gelatin matrix. The blocks were then cryoprotected through 3 cycles of 30% sucrose for 3–4 days each. The blocks were then flash-frozen using dry ice/isomethylpentane, and 40 μm serial sections were cut using a freezing microtome (Nagamoto-Combs et al., 2016). Serial sections (separated by a 960 μm gap) were subjected to antigen retrieval (80% formic acid for 20 minutes) and immunostained using anti-Aβ (D54D2) at a dilution of 1:1000 followed by incubation with biotinylated secondary antibody (1:2000 dilution; Vector Laboratories) and avidin/biotin solution (Vector ABC kit). Immunoreactivity was visualized using Vector VIP as the chromogen. The

slides were dehydrated and coverslipped using Permount (National Diagnostics) following a standard dehydrating procedure through a series of ethanol concentrations and Histo-Clear (National Diagnostics). Images were taken using an upright Leica DM1000 microscope and Leica DF320 digital camera system.

2.8. Biochemical analyses of brain tissue

Flash-frozen parietal cortices from the left brain hemispheres were lysed in radioimmunoprecipitation assay (RIPA) buffer and quantitated using a bicinchoninic acid assay (Pierce, ThermoFisher Scientific). For Aβ ELISAs, RIPA lysates were considered soluble fractions. For insoluble fractions, tissue pellets from RIPA lysates were further lysed in guanidine hydrochloride and quantitated. Aβ 1–40 and Aβ 1–42 levels in both soluble and insoluble fractions were determined using commercial ELISA kits according to the manufacturer protocol. Aβ concentrations were normalized against total protein, averaged, and plotted ±SEM. For dot blot analysis, RIPA lysates were blotted onto polyvinylidene difluoride membranes and incubated in anti-oligomer (A11), anti-fibril (OC), anti-Aβ (6E10), and anti-α-tubulin antibodies. Antibody binding was detected using enhanced chemiluminescence for detection and optical density values were normalized and averaged (±SEM).

2.9. Intestinal immunohistochemistry

Paraformaldehyde-fixed colon samples were serially cryosectioned at 14 μm thickness. Sections were antigen-retrieved using 80% formic acid (20 minutes) for immunostaining with anti-Aβ antibody. Antibody binding was visualized using the Vector VIP chromogen (Vector Laboratories).

2.10. Aβ ELISA of intestinal tissue

Flash-frozen colons were lysed in RIPA buffer with 50 U/mL DNAse1 (Amresco Inc, Solon, OH, USA). ELISA for Aβ levels was performed as described previously for brain tissue.

2.11. Real-time PCR

Flash-frozen temporal cortices and colons were lysed using QIAzol RNA lysis buffer, and RNA was isolated using the Qiagen RNeasy mini kit according to the manufacturer protocol. For amplification of mRNA for tumor necrosis factor alpha (TNF-α), interleukin-6 (IL-6), interleukin-1β (IL-1β), and lipocalin-2 (Lcn-2), 100 ng of RNA was used as a template for performing real-time PCR using the iTaq Universal SYBR Green One-Step kit (Bio-Rad).

2.12. Statistical analyses

Data are presented as mean ± SEM. Values statistically different were determined using two-way ANOVA by comparing mean values from each condition regardless of age or strain and corrected for multiple comparisons using the Holm-Sidak method.

3. Results

3.1. APP/PS1 and App^{NL-G-F} mice had behavior differences compared with WT mice

To assess spontaneous behavior, mice were subjected to a working memory test using a cross maze. The 3-month-old APP/PS1 and App^{NL-G-F} females but not males had reduced percent

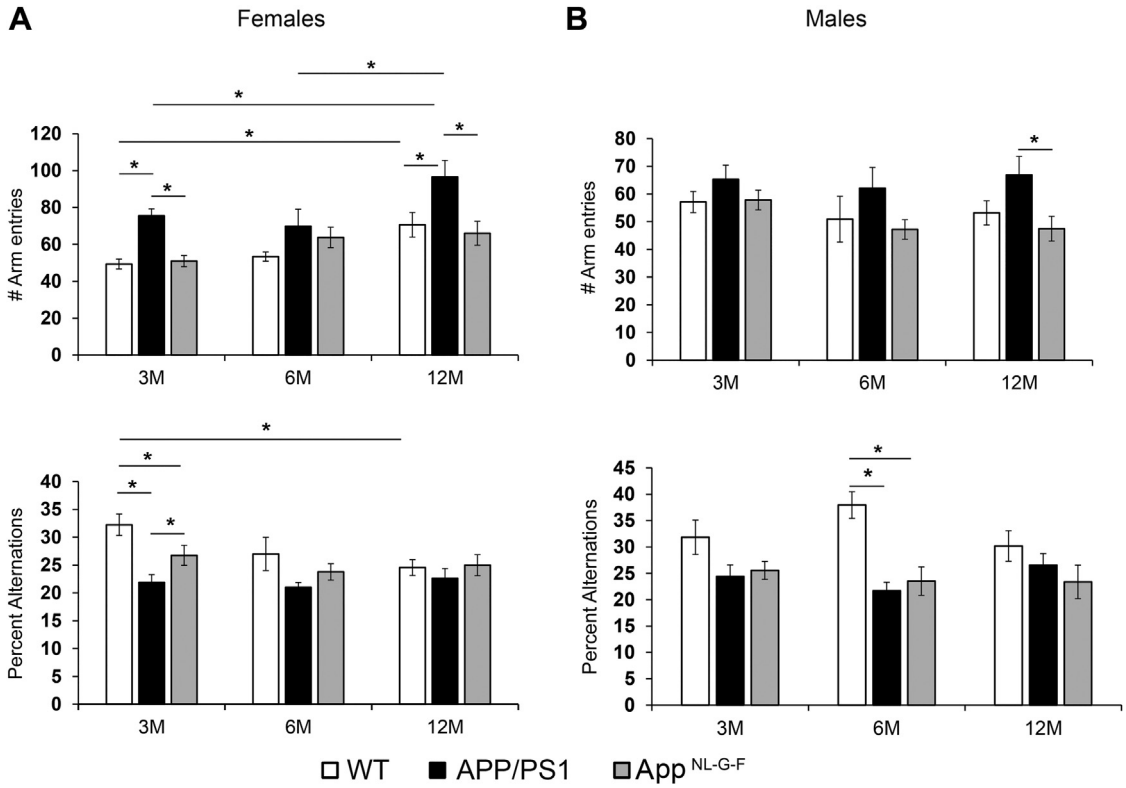

Fig. 1. APP/PS1 and App^{NL-G-F} mice showed working memory differences compared with WT mice. Females (A) and males (B) wild-type (WT), APP/PS1, and App^{NL-G-F} mice at 3, 6, and 12 months of age were subjected to cross-maze testing. Total number of arm entries and number of alternations were recorded, averaged, and plotted ±SEM (n = 10–12). Two-way ANOVA multiple comparisons indicate $F_{4,72} = 1.545$ and $p = 0.198$ (female, percent alternations); $F_{4,84} = 1.121$ and $p = 0.3520$ (female, arm entries); $F_{4,86} = 1.459$ and $p = 0.2218$ (male, percent alternations) and $F_{4,93} = 0.363$ and $p = 0.8344$ (male, arm entries) between all interactions of age and strain. Multiple comparison correction was determined by the Holm-Sidak method, $^*p < 0.05$. Abbreviation: APP, amyloid precursor protein.

alternations, suggesting that they have deficits in working memory at a young age (Fig. 1A). Male APP/PS1, but not male *App*$^{NL\text{-}G\text{-}F}$ mice, developed reduced percent alternations at 6 months of age (Fig. 1B). These data indicate that there are subtle memory deficits in female APP/PS1 and *App*$^{NL\text{-}G\text{-}F}$ mice beginning at a young age (3 months), whereas deficits in male APP/PS1 mice take up to 6 months to present.

3.2. *APP/PS1 mice had increased intestinal permeability and App*$^{NL\text{-}G\text{-}F}$ *had decreased intestinal motility compared with WT mice*

Functionality of the gastrointestinal tract was compared to the behavior changes by performing intestinal motility and permeability assays. Mice were gavaged with 70 kDa FITC-dextran, and motility was quantitated as a measure of percentage gastric emptying and IGC (Fig. 2A). There were no differences observed in the percent gastric emptying between male or female WT, APP/PS1, and *App*$^{NL\text{-}G\text{-}F}$ mice at any age. IGC is a measure of how far the large molecular weight dextran has traveled from the stomach through the small intestine in a given amount of time. A smaller IGC implies slower motility, whereas higher IGC suggests faster intestinal motility. Interestingly, *App*$^{NL\text{-}G\text{-}F}$ females at 3 and 6 months of age had a significantly reduced IGC suggesting slower motility compared with WT and APP/PS1 mice. Motility of 12-month-old *App*$^{NL\text{-}G\text{-}F}$ females was not different compared with WT and APP/PS1 mice. In addition, male WT, APP/PS1, and *App*$^{NL\text{-}G\text{-}F}$ had differences in intestinal motility (Fig. 2A).

For assessing intestinal permeability, mice were gavaged using a smaller molecular weight (4 kDa) FITC-dextran and serum levels were measured 5 hours after gavage (Fig. 2B). In general, APP/PS1 males and females showed trends of increased leakiness compared with WT and *App*$^{NL\text{-}G\text{-}F}$ mice. FITC-dextran levels were significantly

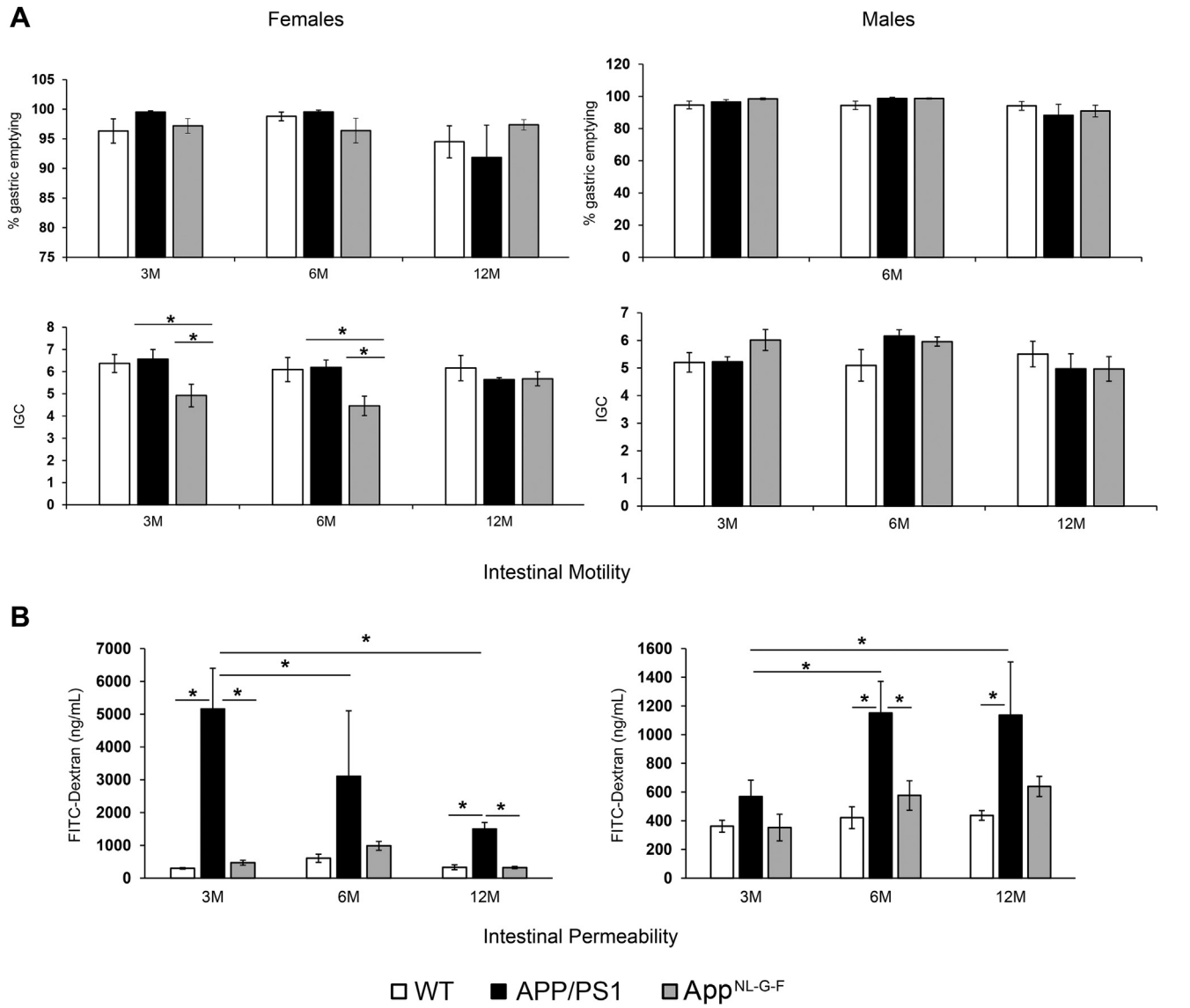

Fig. 2. APP/PS1 mice had increased intestinal permeability and *App*$^{NL\text{-}G\text{-}F}$ had decreased intestinal motility compared with WT mice. Male and female wild-type (WT), APP/PS1, and *App*$^{NL\text{-}G\text{-}F}$ mice at 3, 6, and 12 months of age were subjected to intestinal motility (A) and intestinal permeability (B) assays. For motility assay, percentage gastric emptying and intestinal geometric center were plotted ± SEM (A). For intestinal permeability assay, fluorescence was measured from serum, averaged and plotted ±SEM (B). n = 5–6 per group was used each for intestinal permeability and intestinal motility. Two-way ANOVA multiple comparisons indicate $F_{4,36} = 1.141$ and $p = 0.352$ (female, gastric emptying) $F_{4,36} = 1.473$ and $p = 0.2307$ (female, IGC); $F_{4,39} = 0.9128$ and $p = 0.4661$ (male, gastric emptying); $F_{4,39} = 1.622$ and $p = 0.1881$ (male, IGC); $F_{4,31} = 2.651$ and $p = 0.051$ (female, permeability); and $F_{4,39} = 0.7797$ and $p = 0.545$ (male, permeability) between all interactions of age and strain. Multiple comparison correction was determined by the Holm-Sidak method, $^{*}p < 0.05$. Abbreviations: APP, amyloid precursor protein; IGC, intestinal geometric center.

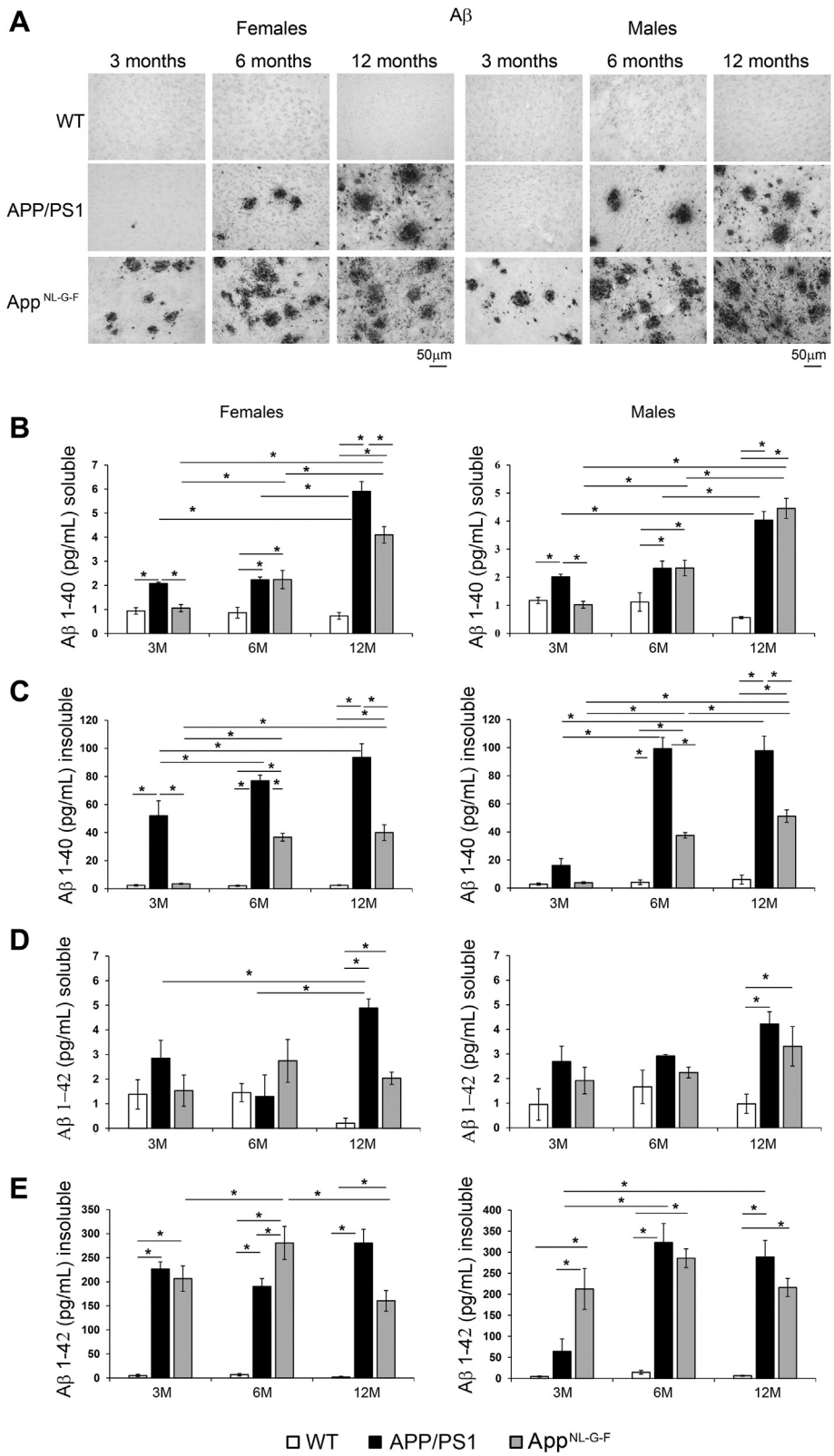

Fig. 3. APP/PS1 and *App*$^{NL-G-F}$ mice showed an age-dependent increase in Aβ immunoreactivity and levels in the brain. (A) Right brain hemispheres from male and female wild-type (WT), APP/PS1, and *App*$^{NL-G-F}$ mice at 3, 6, and 12 months of age were paraformaldehyde-fixed, sectioned, and immunostained using an anti-Aβ antibody. Representative images from 5-6 animals per group are shown at 20 X magnification. The parietal cortex from the left brain hemispheres from all groups of mice were lysed in RIPA buffer to obtain soluble fractions, protein-quantitated, and lysates subjected to Aβ ELISAs. For insoluble Aβ fractions, pellets from RIPA lysates were further lysed in guanidine hydrochloride, and Aβ levels were quantitated using ELISA. Soluble Aβ 1-40 (B), insoluble Aβ 1-40 (C), soluble Aβ 1-42 (D), and insoluble Aβ 1-42 (E) concentrations were normalized, averaged, and plotted ± SEM (n = 5–6). Two-way ANOVA multiple comparisons indicate $F_{4,39}$=18.69 and $p = 0.000$ (female, soluble Aβ 1–40); $F_{4,39} = 5.058$ and $p = 0.0022$ (female, insoluble Aβ 1–40); $F_{4,39} = 5.838$ and $p = 0.0009$ (female, soluble Aβ 1–42); $F_{4,39} = 3.765$ and $p = 0.0110$ (female, insoluble Aβ 1–42); $F_{4,38} = 17.04$ and $p = 0.000$ (male, soluble Aβ 1–40); $F_{4,38} = 6.751$ and $p = 0.000$ (male, insoluble Aβ 1–40); $F_{4,38} = 5.608$ and $p = 0.0012$ (male, soluble Aβ 1–42); and $F_{4,38} = 3.765$ and $p = 0.003$ (male, insoluble Aβ 1–42) between all interactions of age and strain. Multiple comparisons correction was determined by the Holm-Sidak method, $^{*}p < 0.05$. Abbreviations: APP, amyloid precursor protein; Aβ, amyloid beta.

elevated in the serum of 3- and 12-month-old APP/PS1 females and 6- and 12-month-old APP/PS1 males.

3.3. APP/PS1 and App^{NL-G-F} mice showed an age-dependent increase in Aβ immunoreactivity and levels in the brain

To assess the progression of Aβ deposition in the brains with age, sections from WT, APP/PS1, and App^{NL-G-F} mice were immunostained using an anti-Aβ antibody. As expected, both APP/PS1 and App^{NL-G-F} showed an increase in Aβ plaque load with age compared with WT controls in both males and females (Fig. 3A). In addition, deposition of Aβ in the brains of App^{NL-G-F} preceded that of APP/PS1 mice. Aβ immunoreactivity was visible in 3-month-old App^{NL-G-F} mice, whereas it was first observed in APP/PS1 mice at 6 months of age (Fig. 3A).

To validate the immunostaining results, levels of Aβ 1–40 and Aβ 1–42 were quantified in the brains via ELISAs using the parietal cortex (Fig. 3B–E). Both male and female APP/PS1 mice showed an age-dependent increase in soluble and insoluble Aβ 1–40 starting at 3 months of age compared with WT mice (Fig. 3B). In contrast, App^{NL-G-F} mice showed an increase in soluble and insoluble Aβ 1–40 levels starting at 6 months of age (Fig. 3B and C). However, like APP/PS1 mice, App^{NL-G-F} mice had significantly elevated insoluble Aβ 1–42 observable by 3 months of age, whereas soluble Aβ 1–42 levels were not increased until 12 months (Fig. 3D and E). This is in agreement with the Beyreuther/Iberian mutation in the App^{NL-G-F} mice that leads to an increased Aβ42/40 ratio (Guardia-Laguarta et al., 2010; Lichtenthaler et al., 1999). In general, the ELISA data correlated with the Aβ immunohistochemistry, demonstrating an age-dependent increase of Aβ levels in both APP/PS1 and App^{NL-G-F} mice, which corresponded with permeability problems in APP/PS1 mice and intestinal motility issues in App^{NL-G-F} mice (Fig. 2). Parietal cortices were subjected to dot blot analyses using anti-oligomer (A11) and anti-fibril (OC) antibodies (Fig. S1A). APP/PS1 male and female mice showed robustly increased levels of oligomeric and fibrillar protein by 12 months of age (Fig. S1B-C). In comparison, App^{NL-G-F} male and female mice had significantly elevated oligomer and fibril levels at 6 months of age (Fig. S1B-C).

3.4. Colons demonstrated Aβ immunoreactivity in both APP/PS1 and App^{NL-G-F} mice

To begin comparing AD pathology in brains to intestines, we examined Aβ immunoreactivity in colons (Fig. 4). Compared with

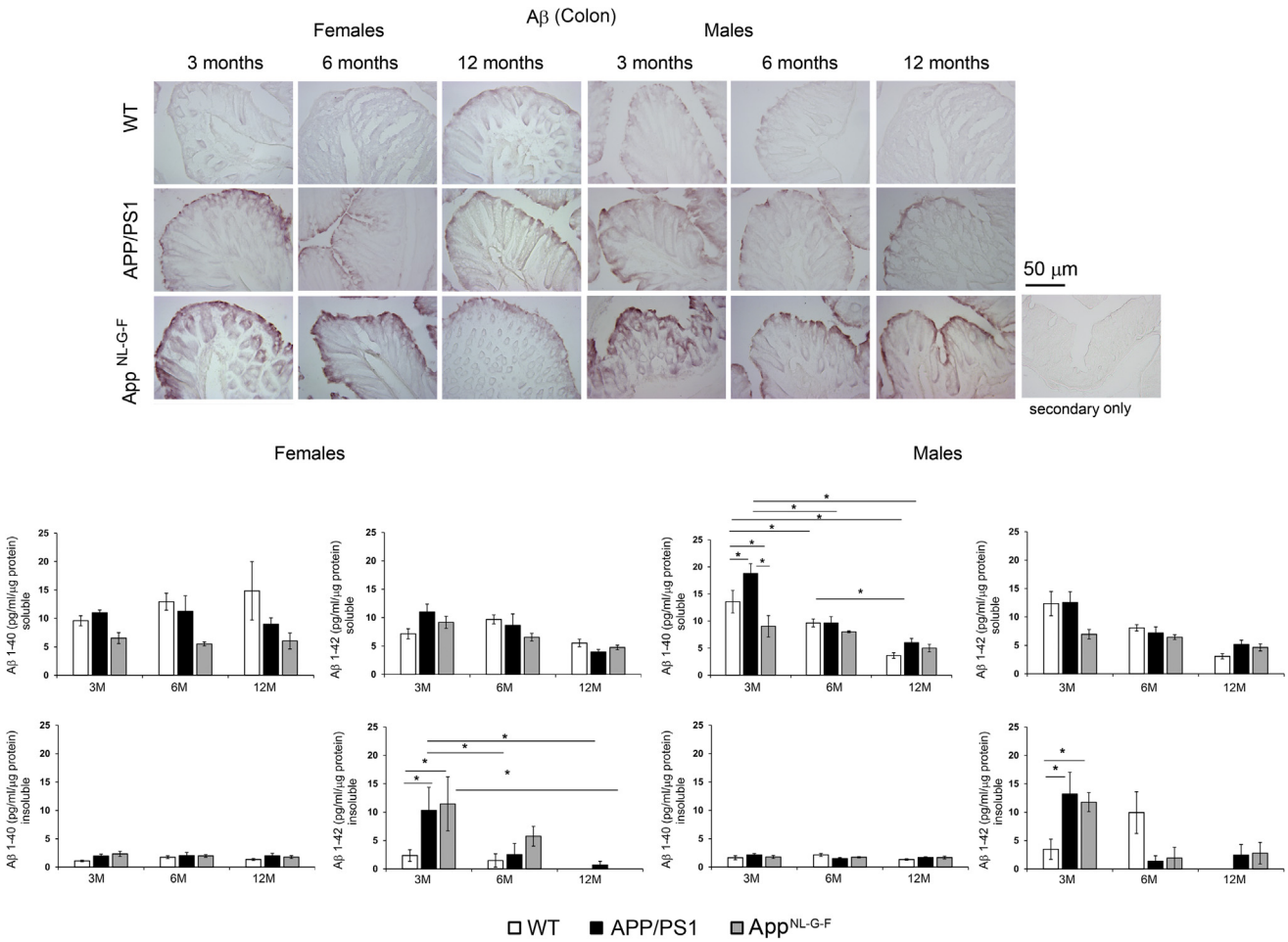

Fig. 4. Colons demonstrated Aβ in both APP/PS1 and App^{NL-G-F} mice. Colons from wild-type (WT), APP/PS1, and App^{NL-G-F} mice were paraformaldehyde-fixed, sectioned, and immunostained using an anti-Aβ antibody. Representative images from 3 animals per group are shown at 20 X magnification. Flash-frozen colons from WT, APP/PS1, and App^{NL-G-F} mice were lysed in RIPA buffer (soluble Aβ fraction) and guanidine hydrochloride (insoluble Aβ fraction). Soluble Aβ 1-40, insoluble Aβ 1-40, soluble Aβ 1-42, and insoluble Aβ 1-42 concentrations were measured using ELISA, normalized, averaged, and plotted ± SEM (n = 5–6). Two-way ANOVA multiple comparisons indicate $F_{4,36} = 1.404$ and $p = 0.2523$ (female, soluble Aβ 1–40); $F_{4,36} = 0.6024$ and $p = 0.6634$ (female, insoluble Aβ 1–40); $F_{4,36} = 2.711$ and $p = 0.045$ (female, soluble Aβ 1–42); $F_{4,36} = 1.263$ and $p = 0.3024$ (female, insoluble Aβ 1–42); $F_{4,36} = 4.021$ and $p = 0.008$ (male, soluble Aβ 1–40) $F_{4,36} = 2.01$ and $p = 0.1138$ (male, insoluble Aβ 1–40); $F_{4,36} = 2.901$ and $p = 0.035$ (male, soluble Aβ 1–42); and $F_{4,34} = 5.088$ and $p = 0.0025$ (male, insoluble Aβ 1–42) between all interactions of age and strain. Multiple comparison correction was determined by the Holm-Sidak method, $^*p < 0.05$. Abbreviations: APP, amyloid precursor protein; Aβ, amyloid beta.

WT mice, 3-, 6-, and 12-month-old APP/PS1 and App^{NL-G-F} mice demonstrated positive Aβ immunostaining. Interestingly, the immunostaining was primarily observed in the epithelium, consistent with our previous work and other reported studies (Galloway et al., 2007, 2009; Puig and Combs, 2013; Puig et al., 2015a). Levels of Aβ 1–40 and Aβ 1–42 in colons from all groups of mice were quantified by Aβ ELISA to measure soluble and insoluble fractions (Fig. 4). Both male and female colons from APP/PS1 and App^{NL-G-F} mice demonstrated significantly elevated levels of insoluble Aβ 1–42 compared with WT mice at the earliest age, 3 months (Fig. 4). Surprisingly, levels of Aβ were not detectable after 3 months of age, suggesting a possible age-associated decrease in production.

3.5. APP/PS1 and App^{NL-G-F} mice had elevated cytokine mRNA in temporal cortices compared with WT controls

Because plaque deposition was observed in the brains of both strains of mice, we next examined the inflammatory state of the brain. Temporal cortices were used to determine mRNA levels of proinflammatory cytokines, TNF-α, IL-6, and IL-1β. Both male and female APP/PS1 and App^{NL-G-F} mice demonstrated increased mRNA levels of the cytokines compared with WT mice with age, particularly TNF-α and IL-1β (Fig. 5). Male and female APP/PS1 mice and male App^{NL-G-F} mice already demonstrated elevated TNF-α mRNA by 3 months of age (Fig. 5) when a memory deficit and increased Aβ levels were also observed but Aβ plaque deposition and gliosis changes were still quite minimal.

3.6. APP/PS1 and App^{NL-G-F} mouse colons had elevated cytokine mRNA in only male mice

Because colons showed increased Aβ in APP/PS1 and App^{NL-G-F} mice consistent with Aβ changes in the brain, we tested whether parallel proinflammatory cytokine changes occurred in the intestines as was observed in the brains. Surprisingly, there were no changes observed in colon cytokine mRNA profiles of female APP/PS1 or App^{NL-G-F} mice compared with WT mice (Fig. 6A). However, like brains, male TNF-α mRNA levels were elevated in both APP/PS1 and App^{NL-G-F} mice compared with WT mice with the APP/PS1 mice already demonstrating an elevation at 3 months of age (Fig. 6B). Male APP/PS1 mice also had elevated IL-6 and IL-1β mRNA at 3 and 6 months of age, demonstrating a complex colonic immune activation in, particularly, the APP/PS1 line. Consistent with the observations from temporal cortex, TNF-α appeared to be a robust inflammation marker at the earliest time point of change in both organs, particularly for male mice. To define an additional marker of intestinal inflammation, colons from all groups of mice were used to quantify mRNA levels of Lcn-2 (Abella et al., 2015). Both male and female APP/PS1 and App^{NL-G-F} mice had significantly increased Lcn-2 mRNA compared with WT mice at 3 months of age, demonstrating this as an additional inflammatory marker for early-stage disease manifestation in the intestines in agreement with elevated insoluble Aβ and TNF-α levels in colons (Fig. 7) (Budzynska et al., 2017; Thorsvik et al., 2018). Male APP/PS1 and App^{NL-G-F} mice maintained the elevated Lcn-2 mRNA levels compared with WT mice up to 6 months of age (Fig. 7). However, by 12 months of age, Lcn-2 mRNA levels were not significantly different between APP/PS1, App^{NL-G-F}, and WT mice (Fig. 7).

4. Discussion

Our previous work demonstrated the presence of APP and Aβ in the intestines of APP/PS1 mice and human AD tissue (Puig et al., 2015a,b). This study was designed to compare the temporal progression of AD-associated changes in the brains and intestines of 2 mouse models of AD, APP/PS1 and App^{NL-G-F} mice. To the best of our knowledge, this is the first report exploring AD pathophysiology

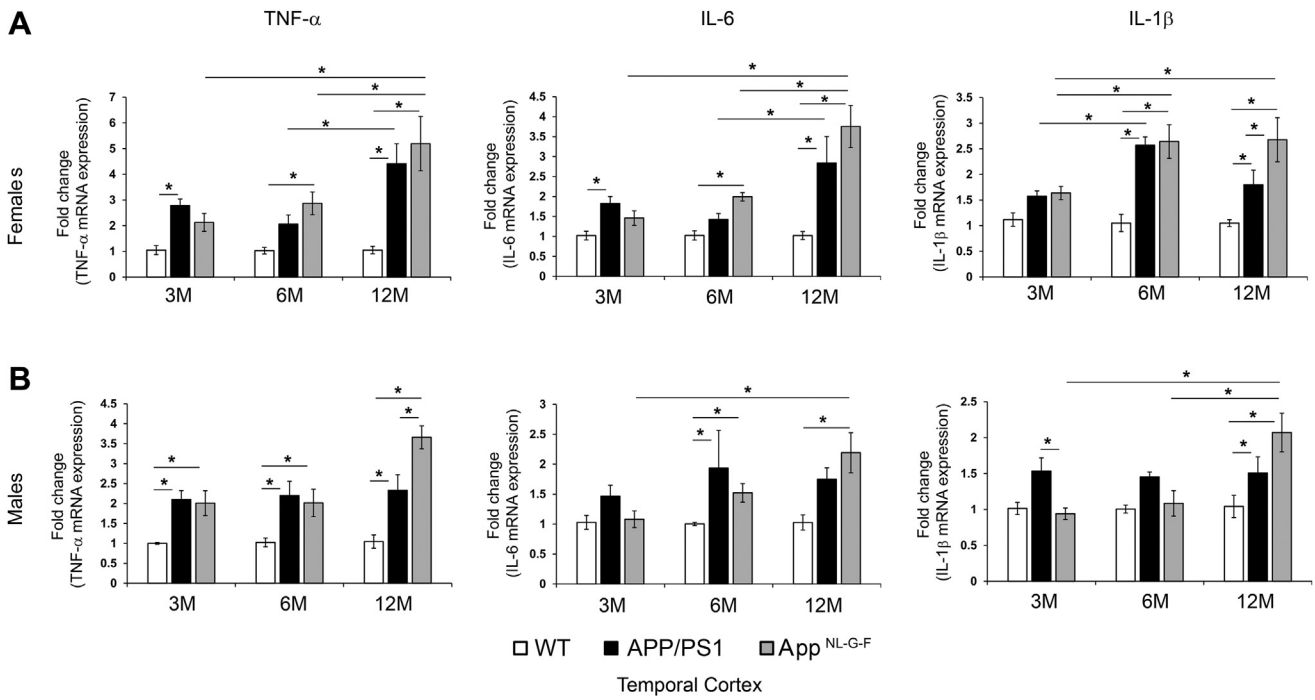

Fig. 5. APP/PS1 and App^{NL-G-F} had elevated cytokine mRNA levels in temporal cortices compared with WT controls. Temporal cortices from WT, APP/PS1, and App^{NL-G-F} female (A) and male (B) mice were lysed in QIAzol and RNA isolated. Real-time PCR for TNF-α, IL-6, and IL-1β from samples were performed, and fold change in mRNA expression was calculated as $2^{-\Delta\Delta Ct}$, averaged, and plotted ±SEM (n = 5). Two-way ANOVA multiple comparisons indicate $F_{4,30} = 2.484$ and $p = 0.064$ (female, TNF-α); $F_{4,31} = 3.37$ and $p = 0.0211$ (female, IL-6); $F_{4,31} = 2.113$ and $p = 0.1029$ (female, IL-1β); $F_{4,34} = 3.446$ and $p = 0.0181$ (male, TNF-α); $F_{4,34} = 1.507$ and $p = 0.222$ (male, IL-6); and $F_{4,34} = 4.476$ and $p = 0.005$ (male, IL-1β) between all interactions of age and strain. Multiple comparison correction was determined by the Holm-Sidak method, $^*p < 0.05$. Abbreviations: APP, amyloid precursor protein; WT, wild type.

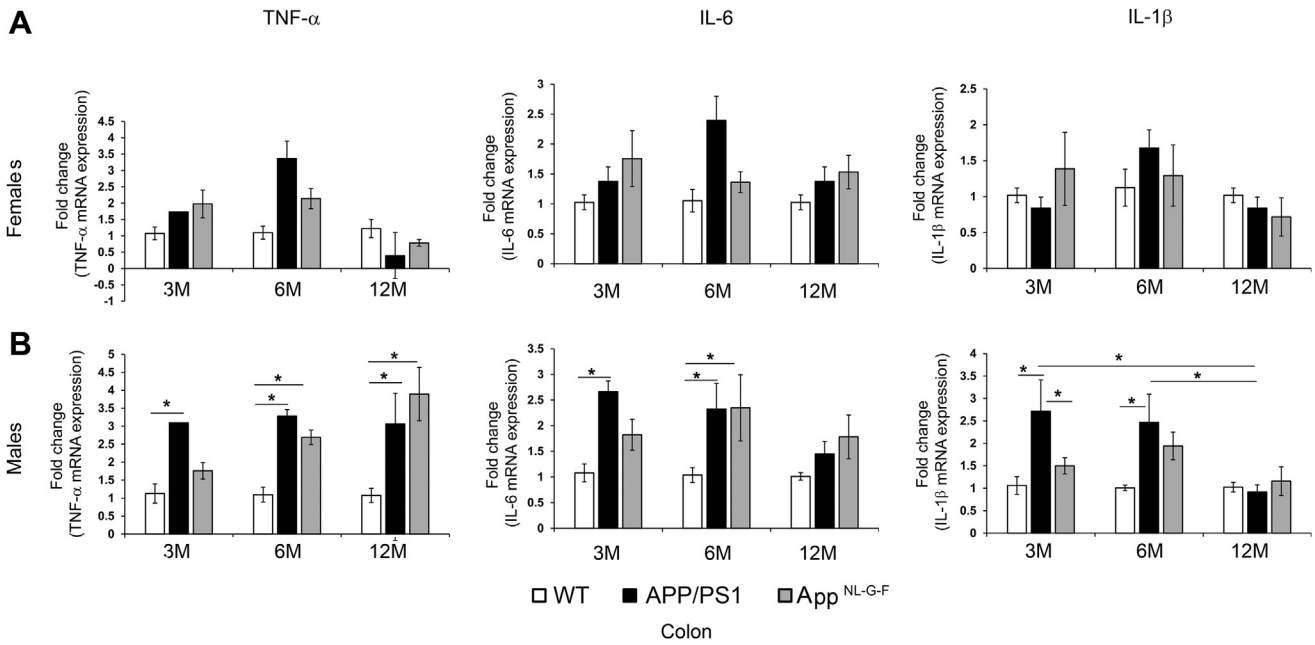

Fig. 6. APP/PS1 and *App*$^{NL-G-F}$ colons had elevated cytokine mRNA levels in the colons of male mice. Flash-frozen colons from WT, APP/PS1, and *App*$^{NL-G-F}$ female (A) and male (B) mice were lysed in QIAzol and RNA isolated. Real-time PCR for TNF-α, IL-6, and IL-1β from samples were performed, and fold change in mRNA expression was calculated as 2^{-}-ΔΔCt, averaged, and plotted ±SEM (n = 5). Two-way ANOVA multiple comparisons indicate $F_{4,36} = 4.703$ and $p = 0.0037$ (female, TNF-α); $F_{4,34} = 2.573$ and $p = 0.0553$ (female, IL-6); $F_{4,36} = 1.108$ and $p = 0.3679$ (female, IL-1β); $F_{4,34} = 2.018$ and $p = 0.1139$ (male, TNF-α); $F_{4,35} = 1.044$ and $p = 0.3987$ (male, IL-6); and $F_{4,36} = 2.058$ and $p = 0.1068$ (male, IL-1β) between all interactions of age and strain. Multiple comparisons correction was determined by the Holm-Sidak method, $^{*}p < 0.05$. Abbreviations: APP, amyloid precursor protein; WT, wild type.

regarding dysfunctional intestinal motility and permeability in transgenic mice. Both brains and intestines correlated with age in terms of Aβ immunoreactivity and inflammatory cytokine changes. All these parameters also correlated with increased intestinal permeability of APP/PS1 mice and somewhat correlated with decreased motility in the *App*$^{NL-G-F}$ mice. The intestinal motility in *App*$^{NL-G-F}$ mice resolved by 12 months of age, and this correlated with the elevated levels of Lcn-2 and IL-1β in these mice. As mentioned earlier, we suggest a brain-gut communication during AD pathophysiology and identify several changes in the colons of AD mouse models that will be useful for monitoring disease progression or understanding the complex multiorgan relationships of AD.

We observed reduced memory performance in male and female mice from both AD lines, with males demonstrating deficiency only at 6 months and females showing a deficit at only 3 months of age. It is unclear why there existed a temporal difference between sexes and why there was no clear age-associated trend. However, it is important to note that the behavioral differences observed in 3-month-old females preceded robust amyloidosis, suggesting that the memory problem may not be directly related to plaque pathology. These data regarding the *App*$^{NL-G-F}$ mice correlate with other published reports of subtle or lack of behavioral deficits (Latif-Hernandez et al., 2017; Whyte et al., 2018). Although others have demonstrated more severe behavior and memory deficits in the *App*$^{NL-G-F}$ mice (Masuda et al., 2016; Saito et al., 2014), this could be attributed to variability of experimental conditions (Whyte et al., 2018). Others have made similar observations regarding a lack of correlation between Aβ plaque deposition and cognitive performance in AD transgenic lines. For example, long-term potentiation was reported to be reduced in male APP/PS1 mice by 3 months of

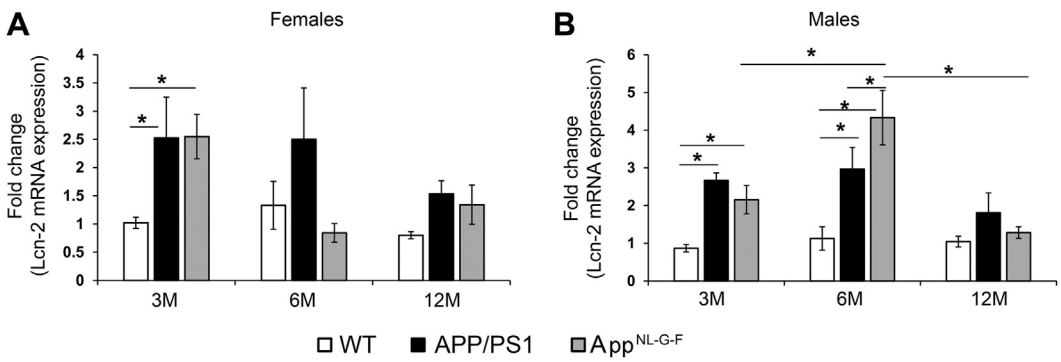

Fig. 7. Colons of male and female APP/PS1 and *App*$^{NL-G-F}$ mice demonstrated elevated mRNA levels of lipocalin-2 (Lcn-2). Flash-frozen colons from WT, APP/PS1, and *App*$^{NL-G-F}$ female (A) and male (B) mice were lysed in QIAzol and RNA isolated. Real-time PCR for Lcn-2 from samples were performed, and fold change in mRNA expression was calculated as 2^{-}-ΔΔCt, averaged, and plotted ±SEM (n = 5). Two-way ANOVA multiple comparisons indicate $F_{4,36} = 1.587$ and $p = 0.1989$ (female, Lcn-2), and $F_{4,33} = 3.672$ and $p = 0.014$ (male, Lcn-2) between all interactions of age and strain. Multiple comparisons correction was determined by the Holm-Sidak method, $^{*}p < 0.05$. Abbreviations: APP, amyloid precursor protein; WT, wild type.

age, correlating with impaired working memory but preceding brain Aβ deposition (Trinchese et al., 2004). A similar study examining an APP/PS1 line demonstrated deficits in Y maze performance at 3 months that was maintained at 6 and 9 months with no decrement in Morris water maze performance at any age in spite of robust plaque deposition at 6 months (Holcomb et al., 1999). However, others have demonstrated using the Tg2576 mouse model of AD and more sensitive Morris water maze testing in a mixed cohort of male and female mice that memory deficits appearing at 6 months of age do correlate with appearance of insoluble Aβ (Westerman et al., 2002). A similar study of mixed male and female mice using an APP/PS1 line demonstrated a positive correlation between plaque load and cognitive dysfunction in the radial arm water maze at 14–16 months of age (Gordon et al., 2001). It appears that the relationship between brain Aβ deposition and behavioral dysfunction in the various transgenic mouse lines will require some standardization of testing approaches across laboratories to arrive at clearer interpretation of any correlation.

Additional age and sex-associated differences were revealed when intestinal activity was quantitated from the mice. Female App^{NL-G-F} mice demonstrated reduced intestinal motility already evident by 3 months of age that may indicate a deficit in smooth muscle contractility preceding robust amyloidosis and gliosis although it was attenuated by 12 months. The lack of motility deficit in App^{NL-G-F} males suggested a more modest intestinal dysfunction compared with females. Surprisingly, the APP/PS1 females had no motility problems although both male and female APP/PS1 mice demonstrated dramatically increased intestinal permeability that existed even at 12 months of age. One possibility for this difference between the APP/PS1 and App^{NL-G-F} mice and the loss of sex difference for the permeability may be due to the fact that overexpression of mutant PS1 in the APP/PS1 mice disrupts the normal role of PS1 in regulating intestinal epithelial cell homeostasis (Nilsberth et al., 1999; Wu et al., 2007). It is clear that γ-secretase activity has a role in regulating intestinal epithelial cell differentiation likely through inhibiting Notch proteolysis (Wong et al., 2004).

Aβ-positive immunoreactivity observed in the colons of APP/PS1 and App^{NL-G-F} mice was observed in the epithelium. Although APP has been observed in the epithelium of the intestines and neurons, we did not observe any robust Aβ plaque-like immunoreactivity (Arai et al., 1991; Cabal et al., 1995; Galloway et al., 2007, 2008, 2009; Joachim et al., 1989; Puig et al., 2015a). Prior work using the APP/PS1 line demonstrated increased intestinal nonplaque-like Aβ immunoreactivity compared with WT controls similar to our observations (Zhou et al., 2017). Van Ginneken et al. also reported no Aβ plaque–like deposition using a Thy-1-APP23 AD mouse model (Van Ginneken et al., 2010). One possibility is that the level of APP expression in enteric neurons is lower than in the central nervous system. Based on the pattern of APP immunoreactivity in the epithelial lining, it is possible that any Aβ produced by these cells is being secreted into the lumen. This behavior might explain the lack of Aβ deposition within the mucosa/submucosa in the AD lines. Indeed, our prior work using the human epithelial cell line derived from colorectal adenocarcinoma, Caco-2 cells, demonstrated the ability of these cells to secrete Aβ on lipopolysaccharide stimulation (Puig et al., 2015b). Another possibility for no Aβ deposition in the intestines could be due to lack of processing of APP to Aβ. For instance, we previously demonstrated the inability of pancreatic islet cells to secrete Aβ in spite of mutant APP expression correlating with limited expression of BACE1 (Kulas et al., 2017). It is clear that intestinal APP is primarily of the larger isoforms also offering the possibility of alternative processing from the brain predominate APP695 (Yamada et al., 1989).

We appreciate that there are significant differences between the amyloidosis models we have examined and human AD. However, in humans, there are intestinal changes that occur with disease. Constipation is a common symptom of elderly dementia patients although it is unclear whether enteric neuron loss is a part of the dementing disease process (Bassotti et al., 2007; Sandman et al., 1983). A study of 4 million U.S. military veterans demonstrated a significant association of AD with the volvulus, impaction of the intestine, constipation, and megacolon (Sonnenberg et al., 1994). In addition, impaired cortical control of swallowing in patients with AD appears to precede late disease stage–associated dysphagia (Humbert et al., 2010). There are also histologic demonstrations of intestinal aspects of disease. Similar to our findings (Puig et al., 2015a), diffuse Aβ immunostaining in AD intestines has been reported (Joachim et al., 1989). Others have also shown robust tau expression within particularly the human sigmoid colon (Dugger et al., 2016). Although we previously noted clear phospho-tau immunoreactivity in AD colons (Puig et al., 2015a), work by others failed to demonstrate tau pathology in AD intestines using the ALZ-50 antibody, suggesting that epitope-specific changes in tau must be considered when assessing enteric changes (Shankle et al., 1993). Finally, a study of 4 individuals with Down syndrome supported a hypothesis of intestinal malabsorption as a component of the condition (Abalan et al., 1990).

Our study aimed to identify peripheral biomarkers that, with further human tissue analyses, might be translated into means of early disease diagnosis using stool analyses or colonoscopy. We identified changes in TNF-α, Aβ, and Lcn-2 levels as colonic changes in the AD mice suitable for identifying a diseased state. Although we do not rule out the possibility of these changes in other intestinal disorders (Abella et al., 2015; Braegger et al., 1992), it is possible that a panel of specific changes might be feasible for differentiating AD from other conditions.

Disclosure

The authors have no actual or potential conflicts of interest.

Acknowledgements

The authors would like to thank Dr. Kendra Puig, Dr. Harpreet Kaur, Lane Vendsel, Danielle Germundson, Mona Sohrabi, Dr. Joshua Kulas, and Nicholas Smith for experimental support. This research was supported by NIH, USA grants RO1AG048993, P20GM113123, and P20GM103442.

Appendix A. Supplementary data

Supplementary data to this article can be found online at https://doi.org/10.1016/j.neurobiolaging.2019.05.025.

References

Abalan, F., Jouan, A., Weerts, M.T., Solles, C., Brus, J., Sauneron, M.F., 1990. A study of digestive absorption in four cases of Down's syndrome. Down's syndrome, malnutrition, malabsorption, and Alzheimer's disease. Med. Hypotheses 31, 35–38.

Abella, V., Scotece, M., Conde, J., Gomez, R., Lois, A., Pino, J., Gomez-Reino, J.J., Lago, F., Mobasheri, A., Gualillo, O., 2015. The potential of lipocalin-2/NGAL as biomarker for inflammatory and metabolic diseases. Biomarkers 20, 565–571.

Akiyama, H., McGeer, P.L., 1990. Brain microglia constitutively express beta-2 integrins. J. Neuroimmunol 30, 81–93.

Akiyama, H., Mori, H., Saido, T., Kondo, H., Ikeda, K., McGeer, P.L., 1999. Occurrence of the diffuse amyloid beta-protein (Abeta) deposits with numerous Abeta-containing glial cells in the cerebral cortex of patients with Alzheimer's disease. Glia 25, 324–331.

Arai, H., Lee, V.M., Messinger, M.L., Greenberg, B.D., Lowery, D.E., Trojanowski, J.Q., 1991. Expression patterns of beta-amyloid precursor protein (beta-APP) in neural and nonneural human tissues from Alzheimer's disease and control subjects. Ann. Neurol. 30, 686–693.

Aube, A.C., Cabarrocas, J., Bauer, J., Philippe, D., Aubert, P., Doulay, F., Liblau, R., Galmiche, J.P., Neunlist, M., 2006. Changes in enteric neurone phenotype and intestinal functions in a transgenic mouse model of enteric glia disruption. Gut 55, 630–637.
Bassotti, G., Villanacci, V., Fisogni, S., Cadei, M., Di Fabio, F., Salerni, B., 2007. Apoptotic phenomena are not a major cause of enteric neuronal loss in constipated patients with dementia. Neuropathol. 27, 67–72.
Braegger, C.P., Nicholls, S., Murch, S.H., Stephens, S., MacDonald, T.T., 1992. Tumour necrosis factor alpha in stool as a marker of intestinal inflammation. Lancet 339, 89–91.
Budzynska, A., Gawron-Kiszka, M., Nowakowska-Dulawa, E., Spiewak, J., Lesinska, M., Kukla, M., Waluga, M., Hartleb, M., 2017. Serum neutrophil gelatinase-associated lipocalin (NGAL) correlates with clinical and endoscopic activity in ulcerative colitis but fails to predict activity in Crohn's disease. J. Physiol. Pharmacol. 68, 859–865.
Cabal, A., Alonso-Cortina, V., Gonzalez-Vazquez, L.O., Naves, F.J., Del Valle, M.E., Vega, J.A., 1995. beta-Amyloid precursor protein (beta APP) in human gut with special reference to the enteric nervous system. Brain Res. Bull 38, 417–423.
Camilleri, M., Cowen, T., Koch, T.R., 2008. Enteric neurodegeneration in ageing. Neurogastroenterol Motil. 20, 185–196.
Combs, C.K., Johnson, D.E., Cannady, S.B., Lehman, T.M., Landreth, G.E., 1999. Identification of microglial signal transduction pathways mediating a neurotoxic response to amyloidogenic fragments of beta-amyloid and prion proteins. J. Neurosci. 19, 928–939.
Dugger, B.N., Whiteside, C.M., Maarouf, C.L., Walker, D.G., Beach, T.G., Sue, L.I., Garcia, A., Dunckley, T., Meechoovet, B., Reiman, E.M., Roher, A.E., 2016. The presence of select tau species in human peripheral tissues and their relation to Alzheimer's disease. J. Alzheimers Dis. 51, 345–356.
Everhart, J.E., Ruhl, C.E., 2009a. Burden of digestive diseases in the United States part I: overall and upper gastrointestinal diseases. Gastroenterology 136, 376–386.
Everhart, J.E., Ruhl, C.E., 2009b. Burden of digestive diseases in the United States part II: lower gastrointestinal diseases. Gastroenterology 136, 741–754.
Fukui, H., Diaz, F., Garcia, S., Moraes, C.T., 2007. Cytochrome c oxidase deficiency in neurons decreases both oxidative stress and amyloid formation in a mouse model of Alzheimer's disease. Proc. Natl. Acad. Sci. U. S. A. 104, 14163–14168.
Galloway, S., Jian, L., Johnsen, R., Chew, S., Mamo, J.C., 2007. beta-amyloid or its precursor protein is found in epithelial cells of the small intestine and is stimulated by high-fat feeding. J. Nutr. Biochem. 18, 279–284.
Galloway, S., Pallebage-Gamarallage, M.M., Takechi, R., Jian, L., Johnsen, R.D., Dhaliwal, S.S., Mamo, J.C., 2008. Synergistic effects of high fat feeding and apolipoprotein E deletion on enterocytic amyloid-beta abundance. Lipids Health Dis. 7, 15.
Galloway, S., Takechi, R., Pallebage-Gamarallage, M.M., Dhaliwal, S.S., Mamo, J.C., 2009. Amyloid-beta colocalizes with apolipoprotein B in absorptive cells of the small intestine. Lipids Health Dis. 8, 46.
Gordon, M.N., King, D.L., Diamond, D.M., Jantzen, P.T., Boyett, K.V., Hope, C.E., Hatcher, J.M., DiCarlo, G., Gottschall, W.P., Morgan, D., Arendash, G.W., 2001. Correlation between cognitive deficits and Abeta deposits in transgenic APP+PS1 mice. Neurobiol. Aging 22, 377–385.
Goyal, R.K., Hirano, I., 1996. The enteric nervous system. N. Engl. J. Med. 334, 1106–1115.
Guardia-Laguarta, C., Pera, M., Clarimon, J., Molinuevo, J.L., Sanchez-Valle, R., Llado, A., Coma, M., Gomez-Isla, T., Blesa, R., Ferrer, I., Lleo, A., 2010. Clinical, neuropathologic, and biochemical profile of the amyloid precursor protein I716F mutation. J. Neuropathol. Exp. Neurol. 69, 53–59.
Holcomb, L.A., Gordon, M.N., Jantzen, P., Hsiao, K., Duff, K., Morgan, D., 1999. Behavioral changes in transgenic mice expressing both amyloid precursor protein and presenilin-1 mutations: lack of association with amyloid deposits. Behav. Genet. 29, 177–185.
Humbert, I.A., McLaren, D.G., Kosmatka, K., Fitzgerald, M., Johnson, S., Porcaro, E., Kays, S., Umoh, E.O., Robbins, J., 2010. Early deficits in cortical control of swallowing in Alzheimer's disease. J. Alzheimers Dis. 19, 1185–1197.
Jankowsky, J.L., Slunt, H.H., Ratovitski, T., Jenkins, N.A., Copeland, N.G., Borchelt, D.R., 2001. Co-expression of multiple transgenes in mouse CNS: a comparison of strategies. Biomol. Eng. 17, 157–165.
Jankowsky, J.L., Fadale, D.J., Anderson, J., Xu, G.M., Gonzales, V., Jenkins, N.A., Copeland, N.G., Lee, M.K., Younkin, L.H., Wagner, S.L., Younkin, S.G., Borchelt, D.R., 2004. Mutant presenilins specifically elevate the levels of the 42 residue beta-amyloid peptide in vivo: evidence for augmentation of a 42-specific gamma secretase. Hum. Mol. Genet. 13, 159–170.
Joachim, C.L., Mori, H., Selkoe, D.J., 1989. Amyloid beta-protein deposition in tissues other than brain in Alzheimer's disease. Nature 341, 226–230.
Johanson, J.F., Sonnenberg, A., Koch, T.R., McCarty, D.J., 1992. Association of constipation with neurologic diseases. Dig. Dis. Sci. 37, 179–186.
Kang, J., Lemaire, H.G., Unterbeck, A., Salbaum, J.M., Masters, C.L., Grzeschik, K.H., Multhaup, G., Beyreuther, K., Muller-Hill, B., 1987. The precursor of Alzheimer's disease amyloid A4 protein resembles a cell-surface receptor. Nature 325, 733–736.
Kulas, J.A., Puig, K.L., Combs, C.K., 2017. Amyloid precursor protein in pancreatic islets. J. Endocrinol. 235, 49–67.
Latif-Hernandez, A., Shah, D., Craessaerts, K., Saido, T., Saito, T., De Strooper, B., Van der Linden, A., D'Hooge, R., 2017. Subtle behavioral changes and increased prefrontal-hippocampal network synchronicity in APP(NL-G-F) mice before prominent plaque deposition. Behav. Brain Res. 364, 431–441.
Lichtenthaler, S.F., Wang, R., Grimm, H., Uljon, S.N., Masters, C.L., Beyreuther, K., 1999. Mechanism of the cleavage specificity of Alzheimer's disease gamma-secretase identified by phenylalanine-scanning mutagenesis of the transmembrane domain of the amyloid precursor protein. Proc. Natl. Acad. Sci. U S A. 96, 3053–3058.
Masuda, A., Kobayashi, Y., Kogo, N., Saito, T., Saido, T.C., Itohara, S., 2016. Cognitive deficits in single app knock-in mouse models. Neurobiol. Learn Mem. 135, 73–82.
Nagamoto-Combs, K., Manocha, G.D., Puig, K., Combs, C.K., 2016. An improved approach to align and embed multiple brain samples in a gelatin-based matrix for simultaneous histological processing. J. Neurosci. Methods 261, 155–160.
Nilsberth, C., Luthman, J., Lannfelt, L., Schultzberg, M., 1999. Expression of presenilin 1 mRNA in rat peripheral organs and brain. Histochem. J. 31, 515–523.
Nilsson, P., Saito, T., Saido, T.C., 2014. New mouse model of Alzheimer's. ACS Chem. Neurosci. 5, 499–502.
Perlmutter, L.S., Barron, E., Chui, H.C., 1990. Morphologic association between microglia and senile plaque amyloid in Alzheimer's disease. Neurosci. Lett. 119, 32–36.
Puig, K.L., Combs, C.K., 2013. Expression and function of APP and its metabolites outside the central nervous system. Exp. Gerontol. 48, 608–611.
Puig, K.L., Lutz, B.M., Urquhart, S.A., Rebel, A.A., Zhou, X., Manocha, G.D., Sens, M., Tuteja, A.K., Foster, N.L., Combs, C.K., 2015a. Overexpression of mutant amyloid-beta protein precursor and presenilin 1 modulates enteric nervous system. J. Alzheimers Dis. 44, 1263–1278.
Puig, K.L., Manocha, G.D., Combs, C.K., 2015b. Amyloid precursor protein mediated changes in intestinal epithelial phenotype in vitro. PLoS One 10, e0119534.
Reiserer, R.S., Harrison, F.E., Syverud, D.C., McDonald, M.P., 2007. Impaired spatial learning in the APPSwe + PSEN1DeltaE9 bigenic mouse model of Alzheimer's disease. Genes Brain Behav. 6, 54–65.
Roach, M., Christie, J.A., 2008. Fecal incontinence in the elderly. Geriatrics 63, 13–22.
Saito, T., Matsuba, Y., Mihira, N., Takano, J., Nilsson, P., Itohara, S., Iwata, N., Saido, T.C., 2014. Single app knock-in mouse models of Alzheimer's disease. Nat. Neurosci. 17, 661–663.
Saito, T., Matsuba, Y., Yamazaki, N., Hashimoto, S., Saido, T.C., 2016. Calpain activation in Alzheimer's model mice is an artifact of APP and presenilin overexpression. J. Neurosci. 36, 9933–9936.
Sandman, P.O., Adolfsson, R., Hallmans, G., Nygren, C., Nystrom, L., Winblad, B., 1983. Treatment of constipation with high-bran bread in long-term care of severely demented elderly patients. J. Am. Geriatr. Soc. 31, 289–293.
Semar, S., Klotz, M., Letiembre, M., Van Ginneken, C., Braun, A., Jost, V., Bischof, M., Lammers, W.J., Liu, Y., Fassbender, K., Wyss-Coray, T., Kirchhoff, F., Schafer, K.H., 2013. Changes of the enteric nervous system in amyloid-beta protein precursor transgenic mice correlate with disease progression. J. Alzheimers Dis. 36, 7–20.
Shankle, W.R., Landing, B.H., Ang, S.M., Chui, H., Villarreal-Engelhardt, G., Zarow, C., 1993. Studies of the enteric nervous system in Alzheimer disease and other dementias of the elderly: enteric neurons in Alzheimer disease. Mod. Pathol. 6, 10–14.
Sonnenberg, A., Tsou, V.T., Muller, A.D., 1994. The "institutional colon": a frequent colonic dysmotility in psychiatric and neurologic disease. Am. J. Gastroenterol. 89, 62–66.
Sood, A., Warren Beach, J., Webster, S.J., Terry, A.V., Buccafusco, J.J., 2007. The effects of JWB1-84-1 on memory-related task performance by amyloid Abeta transgenic mice and by young and aged monkeys. Neuropharmacology 53, 588–600.
Styren, S.D., Civin, W.H., Rogers, J., 1990. Molecular, cellular, and pathologic characterization of HLA-DR immunoreactivity in normal elderly and Alzheimer's disease brain. Exp. Neurol. 110, 93–104.
Thorsvik, S., Bakke, I., van Beelen Granlund, A., Royset, E.S., Damas, J.K., Ostvik, A.E., Sandvik, A.K., 2018. Expression of Neutrophil Gelatinase-Associated Lipocalin (NGAL) in the Gut in Crohn's Disease. Cell Tissue Res. 374, 339–348.
Trinchese, F., Liu, S., Battaglia, F., Walter, S., Mathews, P.M., Arancio, O., 2004. Progressive age-related development of Alzheimer-like pathology in APP/PS1 mice. Ann. Neurol. 55, 801–814.
Trojanowski, J.Q., Vandeerstichele, H., Korecka, M., Clark, C.M., Aisen, P.S., Petersen, R.C., Blennow, K., Soares, H., Simon, A., Lewczuk, P., Dean, R., Siemers, E., Potter, W.Z., Weiner, M.W., Jack Jr., C.R., Jagust, W., Toga, A.W., Lee, V.M., Shaw, L.M., 2010. Update on the biomarker core of the Alzheimer's disease neuroimaging initiative subjects. Alzheimers Dement 6, 230–238.
Van Ginneken, C., Schafer, K.H., Van Dam, D., Huygelen, V., De Deyn, P.P., 2010. Morphological changes in the enteric nervous system of aging and APP23 transgenic mice. Brain Res. 1378, 43–53.
Van Ginneken, C., Schafer, K.H., Van Dam, D., Huygelen, V., De Deyn, P.P., 2011. Morphological changes in the enteric nervous system of aging and APP23 transgenic mice. Brain Res. 1378, 43–53.
von Boyen, G.B., Reinshagen, M., Steinkamp, M., Adler, G., Kirsch, J., 2002. Enteric nervous plasticity and development: dependence on neurotrophic factors. J. Gastroenterol. 37, 583–588.
Wegiel, J., Wang, K.C., Imaki, H., Rubenstein, R., Wronska, A., Osuchowski, M., Lipinski, W.J., Walker, L.C., LeVine, H., 2001. The role of microglial cells and astrocytes in fibrillar plaque evolution in transgenic APP(SW) mice. Neurobiol. Aging 22, 49–61.
Weiner, M.W., Veitch, D.P., Aisen, P.S., Beckett, L.A., Cairns, N.J., Green, R.C., Harvey, D., Jack, C.R., Jagust, W., Liu, E., Morris, J.C., Petersen, R.C., Saykin, A.J., Schmidt, M.E., Shaw, L., Siuciak, J.A., Soares, H., Toga, A.W., Trojanowski, J.Q., 2010. The Alzheimer's disease neuroimaging initiative: a review of papers published since its inception. Alzheimers Dement 8 (1 Suppl), S1–S68.
Westerman, M.A., Cooper-Blacketer, D., Mariash, A., Kotilinek, L., Kawarabayashi, T., Younkin, L.H., Carlson, G.A., Younkin, S.G., Ashe, K.H., 2002. The relationship

between Abeta and memory in the Tg2576 mouse model of Alzheimer's disease. J. Neurosci. 22, 1858–1867.
Whyte, L.S., Hemsley, K.M., Lau, A.A., Hassiotis, S., Saito, T., Saido, T.C., Hopwood, J.J., Sargeant, T.J., 2018. Reduction in open field activity in the absence of memory deficits in the App(NL-G-F) knock-in mouse model of Alzheimer's disease. Behav. Brain Res. 336, 177–181.
Wisniewski, H.M., Wegiel, J., Wang, K.C., Lach, B., 1992. Ultrastructural studies of the cells forming amyloid in the cortical vessel wall in Alzheimer's disease. Acta Neuropathol. 84, 117–127.
Wong, G.T., Manfra, D., Poulet, F.M., Zhang, Q., Josien, H., Bara, T., Engstrom, L., Pinzon-Ortiz, M., Fine, J.S., Lee, H.J., Zhang, L., Higgins, G.A., Parker, E.M., 2004. Chronic treatment with the gamma-secretase inhibitor LY-411,575 inhibits beta-amyloid peptide production and alters lymphopoiesis and intestinal cell differentiation. J. Biol. Chem. 279, 12876–12882.
Wu, S., Rhee, K.J., Zhang, M., Franco, A., Sears, C.L., 2007. Bacteroides fragilis toxin stimulates intestinal epithelial cell shedding and gamma-secretase-dependent E-cadherin cleavage. J. Cell Sci 120 (Pt 11), 1944–1952.
Yamada, T., Sasaki, H., Dohura, K., Goto, I., Sakaki, Y., 1989. Structure and expression of the alternatively-spliced forms of mRNA for the mouse homolog of Alzheimer's disease amyloid beta protein precursor. Biochem. Biophys. Res. Commun. 158, 906–912.
Zhou, Y.L., Du, Y.F., Du, H., Shao, P., 2017. Insulin resistance in Alzheimer's disease (AD) mouse intestinal macrophages is mediated by activation of JNK. Eur. Rev. Med. Pharmacol. Sci. 21, 1787–1794.